Fermions, criticality and superconductivity

She, J.H.

Chapter 6

Measuring the Pair Susceptibility Directly

6.1 Introduction

Dynamical correlation functions provide crucial insights for the understanding of strongly correlated electron systems. By measuring the wavevector- and frequency-dependent magnetic susceptibility, inelastic neutron scattering has become one of the most powerful tools in characterizing magnetism. In these experiments, the beam of scattering external particles couple to the order parameter of the system, in the case of magnetism the spin density of the sample, and the resulting differential scattering cross-section is a direct measure of the autocorrelation function of the order parameter.

For superconductivity, one would ideally also like to measure the susceptibility associated with the order parameter. However, the superconducting pairing order parameter Δ is off-diagonal in particle number space, $\Delta \sim \langle c_\downarrow c_\uparrow \rangle$, and nature does not endow us with an external electromagnetic field that couples directly to the order parameter, like it does for magnetism. A probe of the 'pairing' susceptibility thus always requires an *indirect* measurement.

Such an indirect probe has been known for 40 years. Based on the Josephson effect, in which the order parameters of two superconductors are coupled to each other, in 1970 Ferrell [276] and Scalapino [277] suggested a superconductor-insulator-normal (SIN) tunneling setup in which a strong superconductor acts as an effective external probe for a normal metallic state above its superconducting transition temperature T_c; the fluctuating pair field of the metal is coupled to

the rigid pair-field of the strong superconductor, and this leads to an additional contribution to the total tunneling current, on top of the well-known SIN-junction quasiparticle current. This additional tunneling current is proportional to the imaginary part of the pair(ing) susceptibility of the pairing order parameter of the metallic state (see also [282]).

This scheme has been used to study the pair fluctuations near the superconducting transition temperature. A divergence in the pair susceptibility is universally expected as the phase transition is approached, and a 'relaxational' peak characteristic for Gaussian fluctuations was indeed confirmed experimentally very early on in the work by Goldman and collaborators [278] in aluminum and lead (i.e., conventional s-wave materials), and much more recent also in junctions of d-wave cuprates [283].

Up to now, all the efforts on the pair tunneling experiments have been confined to the region *near* T_c. The pair susceptibility at higher temperatures may have been ignored because for conventional Fermi liquids it is expected to be boring. The main purpose of this chapter is to make it clear to experimentalists that with the recent advances in unconventional superconductivity, especially for systems near the quantum critical points (QCPs), it has become worthwhile to measure the dynamic pair susceptibility away from the transition temperature. The basic point is that the frequency and temperature dependence of the pair susceptibility further away from T_c actually contains important information about the normal state properties of the non-Fermi liquid materials. Such information is vital for the understanding of both the exotic pairing mechanism in such systems and the underlying non-Fermi liquid parent state. Experimentalists have been able to measure the single particle properties of these systems using ARPES and STM, as well as the properties in the particle-hole channel, using for example INS, ESR. However, a direct probe in the particle-particle channel is still lacking, though its importance is obvious, since pairing itself happens in the particle-particle channel. We would like to convince the reader that the pair tunneling experiment actually provides such a highly desired Cooper channel probe .

We will calculate the pair susceptibility for different scenarios of the pairing mechanism for quantum critical metals. Although there exists no proper microscopic description for quantum critical materials, right at the quantum critical point the rules of criticality nevertheless come to our aid, in the sense that we can work with effective models without the need for a microscopic description. We will consider several limiting cases of the whole manifold of possible effective theories. One class of models assumes the separation of the electronic part and the glue part, in which one scenario further assumes that the glue part becomes critical in the quantum critical state; another assumes the electronic part to be critical. The former is best represented by the quantum critical γ-model investigated by Chubukov and collaborators [284]. The latter is the quantum critical BCS (QC-BCS) model that was explored by two of the present authors [121]. There also exist another class of models which do not distinguish between the electronic part and the glue part, only dealing with the bosonic order parameters,

while incorporating scale invariance at high temperature and high frequency. This is the holographic superconductors proposed by Hartnoll, Herzog and Horowitz, for which the superconductor is effectively described by a gravitational theory in one dimension higher [126,285]. We will calculate the dynamic pair susceptibility for these models, in addition to the conventional Fermi liquid BCS model, which is used as a reference point. To our knowledge, this has not been done before. The previous investigations have been focusing on the superconducting transition temperature, for which only the information at zero frequency is needed. The equations we will be solving for the pair correlation functions can be viewed as the finite frequency generalizations of the heavily investigated gap equations, which lie at zero frequency.

In order to experimentally distinguish the various scenarios it is necessary to measure the pair susceptibility away from T_c; to be more precise, a reduced temperature $\tau = (T - T_c)/T_c > 1$ is required. To access such a temperature window clearly demands that the strong superconductor has a significantly larger transition temperature than the quantum critical material of interest. This suggest to consider probing a heavy fermion material at its quantum critical point, where both quantum critical behavior and relatively low T_c ($\simeq 1\,\mathrm{K}$) are expected. The strong side superconductor should have $T_c > 10\mathrm{K}$ to allow for a practical temperature window.

The supposed d-wave symmetry of the order parameter in most materials of interest presents both a challenge and an opportunity. The calculations in this chapter presume s-wave symmetry, but hold equally well for d-wave after projection in the relevant channel. The only real requirement is a non-zero Josephson coupling, in other words a non-zero dc Josephson current at $T = 0$. There is also no hard requirement for the type of interface; a planar junction, point contact, or scanning tunneling tip interface all qualify in essence (for the results in this chapter we work in the tunneling regime). The relaxational peak has been observed in d-wave to d-wave planar junction at very high temperatures 60–80K [283], providing both experimental proof of principle and great promise for lower temperature experiments.

For all the models to be considered in this chapter, we assume a mean field type superconducting phase transition. This is likely true for the quantum critical materials we are interested: optimally doped cuprates and heavy fermions. For underdoped cuprates phase fluctuations are expected to play an important role as well; these are not captured by the current analysis.

The core of this chapter is devoted to numerically determine the pair susceptibility for the three models, as function of frequency and temperature. We will use Eliashberg-like equations throughout this chapter. Eliashberg theory is a fully dynamical theory, where the momentum dependence is assumed to be relatively smooth, and the crucial information is in the frequency dependent part. The solution of these Eliashberg-like equations can only be determined numerically. We extract from the particular parameter sets the general features of the different models. Our main result is summarized graphically in Fig. (6.4) where we

plot the pair susceptibility $\chi_p(\omega, T)$ for the three distinct models (using typical parameters) at the same scale.

The remainder of this chapter is organized as follows. In section 6.2, we give a brief introduction to the tunneling experiment proposed by Ferrell and Scalapino, and realized by Goldman and more recently by Bergeal et al. . In section 6.3 and section 6.4, we turn to theory. Three different models are reviewed in section 6.3, all of which assume electron-glue dualism. These different models are presented in a unified framework using Eliashberg-type integral equations. In section 6.4, we first review the basic idea of the holographic superconductors and then we outline how the pair susceptibility can be calculated by solving the equation of motion for a scalar field. The main results are analyzed in section 6.5. Section 6.6 is devoted to proposing a realistic experiment, including the candidate materials and experimental setup.

6.2 The pair tunneling experiment

The formal definition of the pair susceptibility is as follows,

$$\chi_p(\mathbf{q}, \omega) = -i \int_0^\infty dt e^{i\omega t - 0^+ t} \langle \big[b^\dagger(\mathbf{q}, 0), b(\mathbf{q}, t) \big] \rangle, \tag{6.1}$$

where $b^\dagger(\mathbf{q}, t) = \sum_{\mathbf{k}} c^\dagger_{\mathbf{k}+\mathbf{q}/2,\uparrow}(t) c^\dagger_{-\mathbf{k}+\mathbf{q}/2,\downarrow}(t)$, and $c^{(\dagger)}_{\mathbf{k},\sigma}$ the usual annihilation (creation) operators for electrons with momentum $\mathbf{k}$ and spin σ. For a non-interacting Fermi gas the pair susceptibility can be calculated directly in terms of single particle Green's functions, and gives $\chi_p''(\omega) = \frac{\pi}{2} N(\frac{\omega}{2}) \tanh \frac{\omega}{4T}$. For interacting non-Fermi liquid materials the pair susceptibility is a true two-particle property containing particle-particle pair channel information.

It was realized by Ferrell [276] and worked out further by Scalapino [277] that the pair susceptibility is observable in the tunneling current of an SIN junction. They considered the tunneling regime, i.e., large insulating barrier and consequently small tunneling amplitude γ. In this regime the tunneling current can be calculated perturbatively in the tunneling amplitude. The lowest non-zero contribution to the tunneling current is the well-known linear response result of single quasiparticles tunneling between normal metal and superconductor, of order $|\gamma|^2 \sim R_N$, where R_N is the resistance of the entire junction in a normal state (i.e, NIN junction). This famous, and by now textbook result was observed in the pioneering experiments of Giaever and predicts that at zero temperature (for s-wave superconductor) $I_{\text{tun}} R_N = \sqrt{V^2 - \Delta^2}\, \theta(V - \Delta)$; at finite temperatures there is an exponential suppression of the tunneling current at bias voltages below the gap Δ.

To order $|\gamma|^2$ only isolated quasiparticles can give a non-zero tunneling current. However, at order $|\gamma|^4$ it is possible for Cooper pairs to tunnel, and Cooper pairs are not constraint by the quasiparticle gap Δ. This is what Ferrell and

Scalapino predicted, that there is a contribution to the tunneling current from tunneling Cooper pairs of order $|\gamma|^4$, on top of the quasiparticle tunneling current (contributing at order $|\gamma|^2$ and $|\gamma|^4$). On the normal metal side, this tunneling process corresponds precisely to the imaginary part of the pair susceptibility $\chi_p''(\mathbf{q}=0,\omega)$ where $\hbar\omega = 2eV_{\rm bias}$ [277].

Up to order $|\gamma|^4$, the tunneling current in a SIN is of the form,

$$I_{\rm tun}(V) = I_{\rm qp}(V) + I_{\chi_p''}(V), \tag{6.2}$$

$$I_{\chi_p''}(V) \propto \chi_p''(2eV/\hbar). \tag{6.3}$$

The proportionality factor obviously includes the factor $|\gamma|^4$, but also local densities of state of both S and N materials and effective junction area; since these factors are highly sample-dependent, the overall magnitude of the pair susceptibility contribution to the tunneling current will generally be an experimental fitting parameter. Note that this higher order Cooper pair tunneling process is a second order Josephson effect: if at low temperaturers the regular dc Josephson effect can be observed (i.e., a finite supercurrent at zero bias in SIS configuration), then the higher order tunneling Cooper pair process is likely to occur in the SIN configuration at finite bias.

The pair susceptibility can also be probed at non-zero wave vector $\mathbf{q}$, by applying a magnetic field parallel to the interface surface, which creates the necessary momentum offset of the tunneling pairs [277]. In this chapter we are only concerned with zero momentum $\mathbf{q} = 0$, and we restrict to this case from now on.

The experimental challenge is thus to fabricate a junction that has a discernable second order Josephson tunneling effect. The imaginary part of the pair susceptibility can then be determined up to an unknown overall proportionality factor from the tunneling I-V-curve by subtracting the quasiparticle tunneling current contribution. One may worry that the pair susceptibility signal, of order $|\gamma|^4$, will be so small that it will always drown in the quasiparticle tunneling current signal of order $|\gamma|^2$. There are two reasons why this will likely not be a problem at all: (i) there exist exact expressions for the quasiparticle tunneling current through the Blonders-Tinkham-Klapwijk 'BTK'- formula [286] which has been generalized to d-wave superconductors as well [287]; therefore the quasiparticle tunneling current can be subtracted with rather high precision. And (ii), the quasiparticle tunneling current is rather featureless and suppressed for bias voltages below the gap; close to T_c the pair susceptibility signal is extremely enhanced for $V \ll \Delta$. The true experimental challenge lies in extending the temperature range in which $\chi_p''(\omega)$ can be detected from the total tunneling current to temperatures $(T - T_c)/T_c > 1$.

Goldman and collaborators demonstrated that the proposal by Ferrell and Scalapino is indeed observable in experiment [278]; they considered planar junctions between conventional s-wave superconductors and normal metals, e.g., a aluminum ($T_c \approx 2$K) – aluminum-oxide – lead ($T_c \approx 7$K) NIS interface; this

setup sets an upper bound to the reduced temperature $\tau = (T - T_c)/T_c$ of $\sim (7-2)/2 = 2.5$. They measured tunneling current I-V-curves similar to the ones plotted in Fig. 6.1. They observed a discernable peak with a quasi-Lorentzian line-shape up to $T \approx 3$K (reduced temperature $\tau \approx 0.5$), and at temperature close to T_c, namely at $0.01 < \tau < 0.05$ they found the peak to lie at bias voltage $\omega_{\max} \simeq 8k_B(T - T_c)/\hbar\pi$.

Bergeal et al. recently managed to observe the pair susceptibility at a SIN interface for d-wave materials [283]; they devised a planar junction of an underdoped cuprate ($T_c \approx 60$K) and optimally doped cuprate ($T_c \approx 90$K). This configuration naturally constraints reduced temperature τ to be smaller than 0.5. There are more differences compared with the experiments by Goldman. Instead of directly measuring the tunneling current Bergeal et al. observed the differential conductance. Also, they did not use a generalized BTK formula to subtract the quasiparticle current (instead they noticed that microwave radiation suppressed to peak, and they used this to set the background). The experiment by Bergeal et al. was designed to verify a theoretical prediction by Janko et al. for phase fluctuations in underdoped cuprates [288]; Janko et al. predicted a resonance, instead Bergeal et al. found relaxational behavior. The temperature at which Bergeal et al. performed their experiments are actually rather favorable for our intended target: if the pair susceptibility can be detected at temperatures $T > 60$K the signal should be substantially sharper for temperatures below 10 K, while at the same time allowing reduced temperature to be large. Furthermore, Bergeal et al. observed the relaxational peak that we expect for all different models considered in this chapter. Whether to measure the tunneling current directly or the differential conductance is an experimental trade-off, in principle they carry the same information.

6.3 Pairing mechanisms with electron-glue dualism

The pairing mechanism in quantum critical metals is still under intense debate. Different scenarios have been proposed. It is vital to have an experimental tool to test these scenarios directly. Since superconductivity, i.e., pairing, happens in the Cooper channel, it is surely desirable to be able to measure the Cooper channel directly. Such an experiment has been described in detail in the previous section. The central object that will be measured in such tunneling experiments is the imaginary part of the full dynamical pairing susceptibility. In this section, we will introduce several different scenarios of superconductivity for quantum critical metals. We intend to use these scenarios to represent the different limits of the whole manifold of theories. We study in detail the frequency and temperature evolution of the pair susceptibility in these scenarios. The whole formalism is presented in this section, and the numerical results will be analyzed in the next section.

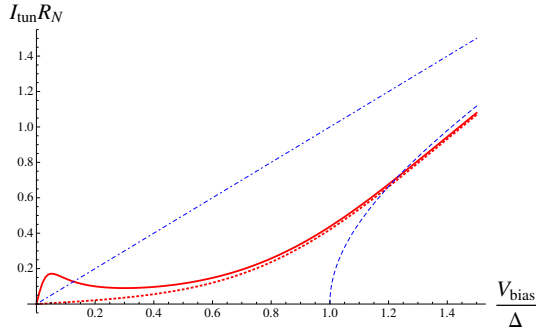

Figure 6.1: Sketch of typical tunneling current $I_{\text{tun}}(V)$ (solid line) as measured in experiments by Goldman. At a temperature $T = \Delta/4$ the usual quasiparticle current for a SIN tunneling junction is given by the dotted line. The difference between the total tunneling current and the quasiparticle current is the pair susceptibility $\chi_p''(\omega = 2eV)$: characterized by a small peak at a relatively low voltage. For reference are plotted as well the zero temperature quasiparticle current (dashed line) and the high temperature linear Ohmic behavior (dotdashed line).

Let us look at the pair susceptibility. The full pair susceptibility contains contributions from all forms of interactions. The general strategy is to separate it into two parts: the electronic part and the glue part. The electronic part is non-singular down to extremely low temperatures. The Coulomb interaction is included in this part. The bosonic glue mediates an attractive electron-electron interaction. It may arise from the coupling of the electrons to lattice distortions. It can also be the collective excitations of the electrons themselves. In some heavy fermion compounds in the vicinity of magnetic quantum phase transitions, magnetic fluctuations may act as glue for superconductivity. For some superconductors, like cuprates, it is questionable whether the glue part is even relevant, since it has a much lower energy scale than that of the electronic interaction, say U and J [289]. We will see later on that in some scenarios the peculiarity of the quantum critical states can lead to the surprising result that even a weak glue can have tremendous effect on superconductivity.

The glue is generally retarded in the sense that its characteristic energy scale ω_b is small compared to the ultraviolet cut-off scale of the electronic part ω_c. With a small Migdal parameter ω_b/ω_c, the electron-glue vertex corrections can then be ignored and the effects of the glue are described by the Migdal-Eliashberg time-dependent mean field theory. And we have the Bethe-Salpeter equation (see Fig. 6.2),

$$\chi(k,k';q) = \chi_0(k,k';q) + u^2 \sum_{k_1,k_2} \chi_0(k,k_1;q) D(k_2-k_1) \chi(k_2,k';q), \qquad (6.4)$$

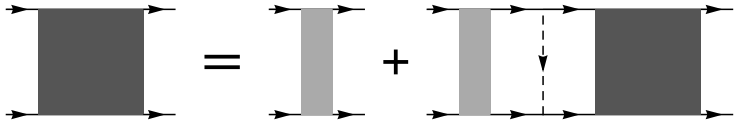

Figure 6.2: Feynman diagram of the Cooper channel Bethe-Salpeter equation. The dark gray square represents the four-point correlation function in the Cooper channel and the light gray rectangle is the corresponding electronic part. The solid lines stand for the electron propagator and the dashed line is the glue propagator.

where $\chi(k,k';q)$ represents the full four-point correlation function with incoming momenta/frequencies $(-k,k+q)$ and outgoing momenta/frequencies $(-k',k'+q)$ and $\chi_0(k,k';q)$ is the corresponding electronic part; $D(p)$ is the glue propagator and u the electron-glue coupling strength taken to be constant below the ultraviolet cut-off scale. The momentum and frequency are grouped in a single symbol here, i.e., four-vector notation $q=(\mathbf{q},\omega)$. The pair susceptibility is obtained from the four-point correlation function by performing a summation over the relative momenta/frequencies, $\chi_p(q)=\sum_{k,k'}\chi(k,k';q)$.

Further simplification can be made by assuming that the pairing problem in quantum critical metals can still be treated within the Eliashberg-type theory, with the electronic vertex operator χ_0 and the glue propagator D strongly frequency dependent, but no substantial momentum dependence. The glue part will only appear in the form of a frequency-dependent pairing interaction $\lambda(\Omega)=\int d^d\mathbf{q}D(\mathbf{q};\Omega)$. A partial summation over the outgoing momenta/frequencies gives the vertex operator $\Gamma(k;q)=\sum_{k'}\chi(k,k';q)$. Also performing the integration over the relative momentum in Γ_0, and taking the total momentum to be vanishing, i.e. $\Gamma_0(\nu;\omega)=\int d\mathbf{k}\Gamma_0(\mathbf{k},\nu;\mathbf{q}=0,\omega)$, we arrive at the final form of the Bethe-Salpeter equation with only (imaginary) frequency arguments,

$$\Gamma(i\nu;i\Omega) \;=\; \Gamma_0(i\nu;i\Omega) \;+\; \mathcal{A}\,\Gamma_0(i\nu;i\Omega)\sum_{\nu'}\lambda(i\nu' \;-\; i\nu)\Gamma(i\nu';i\Omega). \quad (6.5)$$

A further frequency summation over ν yields the pair susceptibility $\chi_p(i\Omega,\mathbf{q}=0)=\sum_\nu\Gamma(i\nu;i\Omega)$ at imaginary frequency $i\Omega$; analytic continuation $i\Omega\to\omega+i\eta$ will give the desired pair susceptibility at real frequency $\chi_p(\omega)$.

The superconducting transition happens when the real part of the full pair susceptibility at $\omega=0$ diverges. The gap equation is the $\omega=0$ limit of the Bethe-Salpeter equation,

$$\Gamma(i\nu)=\Gamma_0(i\nu)+\mathcal{A}\,\Gamma_0(i\nu)\sum_{\nu'}\lambda(i\nu'-i\nu)\Gamma(i\nu'), \quad (6.6)$$

with $\Gamma(i\nu)=\Gamma(i\nu;i\Omega=0)$.

The Bethe-Salpeter equation (6.5) can be solved either by iteration or by direct matrix inversion. The transition temperature T_c is determined by setting the determinant of the kernel equal to zero at zero Matsubara frequency. We will compare three different approaches to pairing in the remainder of this section.

6.3.1 Fermi liquid BCS

We first present as point of reference the case of Fermi liquid BCS. We consider a free Fermi gas, interacting via a normal glue, say an Einstein phonon. The electronic part of the pair susceptibility is simply the convolution of single-particle Green's functions,

$$\chi_0(\mathbf{q}, i\Omega) = \frac{T}{N} \sum_{\mathbf{k},n} G\left(-\mathbf{k}, -i\nu_n\right) G\left(\mathbf{k}+\mathbf{q}, i\nu_n + i\Omega\right). \tag{6.7}$$

For this model, we ignore the self-energy correction, and use the free fermion Green's function $G(\mathbf{k}, i\omega) = 1/(i\omega_n - \varepsilon_{\mathbf{k}})$. The imaginary part of the bare pair susceptibility has the simple form $\chi_0''(\omega) = \frac{1}{\omega_c} \tanh\left(\frac{1}{4}\beta\omega\right)$ at $\mathbf{q} = 0$. Here the Fermi energy acts as the ultraviolet cut-off, with $\omega_c = \frac{2}{\pi N(0)} \simeq E_F$. The bare vertex operator reads

$$\Gamma_0(i\nu_n, i\Omega) = \frac{2T}{\omega_c(2\nu_n + \Omega)} \left[\theta(\nu_n + \Omega) - \theta(-\nu_n)\right], \tag{6.8}$$

with $\theta(x)$ the Heaviside step function. $\Gamma_0(i\nu_n, i\Omega)$ vanishes in the interval $-\Omega < \nu_n < 0$, and decays as $1/\nu_n$ for ν_n large. It is symmetric under the transformation $\nu_n \to -\Omega - \nu_n$. This symmetry can be made more explicit by writing $\Gamma_0(i\nu_n, i\Omega)$ in terms of the relative frequencies $\tilde{\nu}_n = \Omega/2 + \nu_n$,

$$\Gamma_0(i\nu_n, i\Omega) = \frac{T}{\omega_c \tilde{\nu}_n} \left[\theta(\frac{\Omega}{2} + \tilde{\nu}_n) - \theta(\frac{\Omega}{2} - \tilde{\nu}_n)\right]. \tag{6.9}$$

For $i\Omega = 0$, $\Gamma_0(i\nu_n, i\Omega)$ is simply $T/(\omega_c|\nu_n|)$. A BCS-type paring interaction

$$\lambda(\nu' - \nu) = \begin{cases} g/\mathcal{A} & \text{for } |\tilde{\nu}|, |\tilde{\nu}'| < \omega_b, \\ 0 & \text{otherwise,} \end{cases} \tag{6.10}$$

leads to the gap equation

$$1 - g \sum_{|\nu| < \omega_b} \Gamma_0(i\nu_n, \Omega = 0) = 0, \tag{6.11}$$

which gives immediately for the Fermi liquid BCS model an exponentially small transition temperature $T_c \simeq \omega_b \exp\left(-1/\lambda\right)$, with $\lambda = gN(0)$.

We also note that the BCS-type paring interaction (6.10) leads to a simple RPA form for the full pair susceptibility,

$$\chi(\omega) = \frac{\chi_0(\omega)}{1 - g\chi_0(\omega)}, \tag{6.12}$$

where retardation enters through the bare pair susceptibility, $\chi_0(\omega) = \sum_{|\tilde{\nu}|<\omega_b} \Gamma_0(\nu;\omega)$.

However, for the subsequent numerical calculation of the full dynamical pair susceptibility, we will instead use the pairing interaction from a single Einstein phonon,

$$\lambda(i\Omega) = \frac{g}{\mathcal{A}} \frac{\omega_b^2}{\omega_b^2 + \Omega^2}, \tag{6.13}$$

which has the nice property that it is smooth and nonsingular for all frequencies, and does not give extra artificial features in the result.

6.3.2 The Critical Glue Model

Now we will start to consider the new models proposed for quantum critical metals that go beyond the conventional Fermi liquid BCS theory. In this subsection, we will present one class of scenarios that attribute the novelty of unconventional superconductivity in such systems to the peculiar behavior of the glue when approaching the QCP. The glue part is assumed to become critical near the QCP, while the electronic part is still kept a conventional fermion bubble, though with self-energy corrections. We will call such scenarios the critical glue model.

This class of scenarios are arguably best represented by the models introduced by Chubukov and collaborators [284], where they assume that pairing is mediated by a gapless boson, and the pairing interaction is of the power-law form

$$\lambda(i\Omega) = \left(\frac{\Omega_0}{|\Omega|}\right)^{\gamma}. \tag{6.14}$$

Here the exponent γ parameterizes the different models, and it is usually assumed to take values between 0 and 1. For example, an antiferromagnetic QCP gives rise to a pairing interaction with $\gamma = 1/2$, and a ferromagnetic QCP has $\gamma = 1/3$. The pairing interaction has a singular frequency dependence, which makes the pairing problem in such models qualitatively different from that of the Fermi liquid BCS model. The coupling strength is absorbed in the single scale-full parameter Ω_0.

The electronic part of the pair susceptibility is assumed to be still just the convolution of the single particle Green's functions, i.e., of the same form as Eq. (6.7). But now the massless boson also contributes a nontrivial self-energy, $\Sigma(i\omega_n) = i\omega_n \left(\Omega_0/|\omega_n|\right)^{\gamma} S(\gamma, n)$, where $S(\gamma, n) = |n + 1/2|^{\gamma-1} \left[\zeta(\gamma) - \zeta(\gamma, |n + \frac{1}{2}| + \frac{1}{2})\right]$, with $\zeta(\gamma)$ the Riemann zeta function and $\zeta(\gamma, n)$ the generalized Riemann zeta

function. Let us define $Z(\omega_n) = 1 + (\Omega_0/|\omega_n|)^\gamma S(\gamma, n)$. The bare pair susceptibility thus reads

$$\chi_{p,0}(i\Omega) = \frac{T}{N}\sum_{\mathbf{k},\nu_n} \frac{1}{-i\nu_n Z(-\nu_n) - \xi_{\mathbf{k}}} \frac{1}{i(\nu_n+\Omega)Z(\nu_n+\Omega) - \xi_{\mathbf{k}}}. \tag{6.15}$$

And the corresponding bare vertex operator becomes

$$\Gamma_0(i\nu_n, i\Omega) = \frac{2T}{\omega_c[(\nu_n+\Omega)Z(\nu_n+\Omega) + \nu_n Z(-\nu_n)]} \times \\ [\theta((\nu_n+\Omega)Z(\nu_n+\Omega)) - \theta(-\nu_n Z(-\nu_n))]\,. \tag{6.16}$$

With the glue becoming critical, the only scale in such models is Ω_0. And the superconducting transition temperature is proportional to Ω_0, with a model-dependent coefficient, $T_c = A(\gamma)\Omega_0$.

6.3.3 Quantum Critical BCS

In this subsection we will consider another scenario for superconductivity in quantum critical metals, which is orthogonal to the critical glue mode presented in the last subsection. In this approach, the novelty of unconventional superconductivity in such systems is attributed solely to the critical behavior of the electronic part, with the glue part assumed featureless. Hereafter this approach will be dubbed quantum critical BCS (QCBCS) scenario [121].

According to its behavior in the scaling limit, the electronic part of the pair susceptibility $\chi_{p,0}$ was classified into three different categories: marginal, relevant and irrelevant. The prototype of the marginal case is the free Fermi gas, for which the imaginary part of the bare pair susceptibility $\chi''_{p,0}$ is essentially constant at low temperatures. In the QCBCS scenario, the quantum critical metals were assumed to fall into another category tagged as relevant, i.e., $\chi''_{p,0}$ increases when going to lower frequency or lower temperature. More spectral weight is accumulated at lower energy scales, where pairing is more effective. Thus it is much easier to get superconductivity in such models. The gap equation becomes algebraic, and even a weak glue can give rise to a high temperature superconductor. The basic logic behind such construction is the empirical fact the quantum critical metals are more susceptible than Fermi liquid metals. When approaching the QCP, an interaction that was deemed irrelevant initially, takes over and dominates, replacing the QCP by a new stable phase.

A massless boson, as was considered in the critical glue model, modifies the electronic part of the pair susceptibility through self-energy corrections, giving a nice example of an irrelevant pair susceptibility, i.e., $\chi''_{p,0}$ decreases when going to lower frequency or lower temperature. We emphasize that this does not necessarily imply that the critical glue model is ineffective in producing pairing. The massless boson is providing self-energy corrections to single particle Green's

functions and inducing an attractive interaction between electrons at the same time. The two effects compensate, and it is actually possible to produce a high transition temperature.

Coming back to the QCBCS scenario, at zero temperature, the imaginary part of the bare pair susceptibility has the scaling form $\chi''_{p,0}(\omega) \sim \omega^{-\alpha_p}$, with the exponent α_p parameterizing different models; $\alpha_p = 0$, i.e., $\chi''_{p,0}(\omega)$ constant, corresponds to the marginal case. When $\alpha_p > 0$, $\chi''_{p,0}$ increases at lower frequency, describing a relevant pair susceptibility; $\alpha_p < 0$ corresponds to the irrelevant case.

Aiming at the dynamical pairing susceptibility, let us now consider the QCBCS scenario at finite temperature. Temperature breaks conformal invariance and in the euclidean formulation of field theory the imaginary time direction is compactified, leading to the finite size scaling form of the bare pair susceptibility,

$$\chi_{p,0}(\omega, T) = \frac{Z}{T^{\alpha_p}} \mathcal{F}\left(\frac{\omega}{T}\right), \tag{6.17}$$

with the exponent $0 < \alpha_p < 1$, Z a UV renormalization constant and $\mathcal{F}$ a scaling function. The upper bound on α_p stems from unitarity requirements. At zero temperature, this turns into the branch cut as shown above, $\chi_0 \sim \omega^{-\alpha_p}$, while in the opposite high temperature or hydrodynamical regime ($\hbar\omega \ll k_B T$) it takes the form

$$\chi_{p,0}(\omega, T) = \frac{Z'}{T^{\alpha_p}} \frac{1}{1 - i\omega\tau_{\rm rel}}, \tag{6.18}$$

where $\tau_{\rm rel} \approx \hbar/k_B T$.

One example of such a scaling function $\mathcal{F}(\omega/T)$ that possesses the above two limiting forms at low and high temperatures is the following one, borrowed from exact solutions in $1+1$-dimensional conformal field theory,

$$\mathcal{F}''(y) = \sinh(\frac{y}{2}) B^2(s + i\frac{y}{4\pi}, s - i\frac{y}{4\pi}), \tag{6.19}$$

where B is the Euler beta function, and $s = 1/2 - \alpha_p/4$. Another example that results in such a scaling function is a simple generalization of the free fermion vertex operator (6.9),

$$\Gamma_0(i\nu_n, i\Omega) = \frac{(1-\alpha)T}{\omega_c^{1-\alpha} \mathrm{sgn}(\tilde{\nu}_{\rm n}) |\tilde{\nu}_n|^{\alpha+1}} \left[\theta(\frac{\Omega}{2} + \tilde{\nu}_n) - \theta(\frac{\Omega}{2} - \tilde{\nu}_n)\right]. \tag{6.20}$$

One can check that this vertex operator actually leads to a relevant pair susceptibility with $\alpha_p = \alpha$, a power-law tail at high frequency, and the linear hydrodynamic behavior at low frequency. There is a peak at frequencies of order the temperature. We will use this latter one to calculate the full pair susceptibility.

Combining the BCS-type pairing interaction (6.10) and the above vertex operator (6.20) one arrives at an algebraic gap equation characteristic of the QCBCS scenario,

$$1 - 2g \frac{1-\alpha_p}{\omega_c^{1-\alpha_p}} \int_{T_c}^{\omega_b} \frac{d\nu}{\nu^{\alpha_p+1}} = 0, \tag{6.21}$$

As in the Fermi liquid BCS case, we will also use the smooth and nonsingular pairing 'Einstein phonon' interaction (6.13) to calculate the dynamical pair susceptibility in the QCBCS scenario.

6.4 Holographic superconductors

The three different models we considered in the last section all assume the separation of the electronic part and the glue part. There also exist another class of models for which superconductivity is "glueless" and instead driven by the extreme instability of the zero temperature critical state itself. This class of models are based upon the AdS/CFT correspondence of string theory and are called "holographic superconductors" (HS). The simplest model to obtain a holographic superconductor with quite similar behavior to real superconductors was first built in [285, 290] through Einstein gravity which is minimally coupled to a Maxwell field and a charged complex scalar with a potential term. The system is described by the action

$$\mathcal{S}=\int d^4x\sqrt{-g}\Big[R+\frac{6}{L^2}-\frac{1}{4}F_{\mu\nu}F^{\mu\nu}-m^2\Psi^*\Psi-(\nabla^\mu\Psi-iqA^\mu\Psi)^*(\nabla_\mu\Psi-iqA_\mu\Psi)\Big]. \tag{6.22}$$

Here we consider the superconductor to be 2+1 dimensional. A generalization to 3+1 dimension is straightforward.

Below some critical temperature T_c, the charged black hole solutions develop a nonzero static scalar field outside the horizon, which is usually called a nontrivial hair. There are two possible reasons for this instability on the gravity side. One is that the effective mass for the scalar field is $m^2_{\text{eff}}=m^2+q^2g^{tt}A_t^2$. Since the last term is negative, there is a chance that m^2_{eff} becomes sufficiently negative near the horizon to destabilize the scalar field. Furthermore, as one lowers the temperature of a charged black hole, it becomes closer to extremal which means that g_{tt} is closer to developing a double zero at the horizon. So at low temperatures, $|g^{tt}|$ is large and instability becomes strong. Another reason for the instability comes from the fact that at low temperatures the horizon geometry of the near extremal RN black hole has an AdS_2 near-horizon throat. Then an asymptotically stable negative mass squared scalar field can become unstable because the Breitenlohner-Freedman (BF) bound is different for the near horizon AdS_2 and the asymptotic AdS_4. This gives the chance that we can have the condensate even for uncharged scalar field with $q=0$.

The combined effects of these two mechanisms lead the charged black holes to develop scalar hair at low temperatures. According to the AdS/CFT dictionary, on the dual field theory side there is a global U(1) symmetry which corresponds to the U(1) gauge symmetry on the gravity side. From the point of view of the dual field theory, this $U(1)$ symmetry is broken below T_c at a finite charged density because of the condensation of the charged scalar. The complex scalar Ψ

corresponds to the scalar operator of the order parameter $\mathcal{O}$ of the dual field theory. In the following, we focus on the normal state of holographic superconductor which is described by RN-AdS black hole

$$ds^2 = -f(r)dt^2 + \frac{dr^2}{f(r)} + r^2(dx^2+dy^2), \tag{6.23}$$

$$f(r) = r^2 - \frac{1}{r}\left(r_+^3 + \frac{\rho^2}{4r_+}\right) + \frac{\rho^2}{4r^2}, \tag{6.24}$$

$$A = \rho\left(\frac{1}{r_+} - \frac{1}{r}\right)dt, \tag{6.25}$$

The black hole is characterized by two parameters, the location of the horizon r_+ and the charge density ρ. They are related to the mass and charge of RN-AdS black hole respectively. The Hawking temperature of the black hole, which is identified as the temperature of the dual field theory in the AdS/CFT duality, is $T = (3r_+/4\pi)[1-\rho^2/(12r_+^4)]$. When $r\to\infty$, $A_t \to \mu - \rho/r$. Here μ and ρ are identified as the chemical potential and the charge density of the dual field theory respectively. In the following, we fix the charge density to be $\rho_0 = 1$.

Since the dual operator of Ψ is the order parameter, the two-point retarded Green's function of the dual operator for the fluctuation of Ψ gives the pair susceptibility,

$$\chi(\mathbf{k},\omega) = G^R_{\mathcal{O}^\dagger\mathcal{O}}(\mathbf{k},\omega). \tag{6.26}$$

We will calculate the two-point retarded Green's function for the fluctuation of Ψ in the normal phase above the transition temperature T_c, i.e. our calculation is in the RN-AdS black hole background. We consider the zero momentum mode of $\delta\Psi$ and expand it as $\delta\Psi(r,x,t) = \psi(r)e^{-iwt}$. The equation of motion for $\psi(r)$ is

$$\psi'' + \left(\frac{f'}{f} + \frac{2}{r}\right)\psi' + \left(\frac{(w+qA_t)^2}{f^2} - \frac{m^2}{f}\right)\psi = 0. \tag{6.27}$$

Since we are interested in the retarded Green's function, we impose the infalling boundary condition in the near horizon geometry [291], i.e.

$$\psi(r) \simeq (r-r_+)^{-i\frac{w}{4\pi T}} \quad \text{as } r\to r_+. \tag{6.28}$$

Near the boundary, the scalar field goes as

$$\psi(r) \simeq \frac{\psi_-}{r^{\triangle_-}} + \frac{\psi_+}{r^{\triangle_+}} \quad \text{as } r\to\infty, \tag{6.29}$$

where $\triangle_\pm = \frac{3}{2} \pm \nu$ with $\nu = \sqrt{9+4m^2}/2$.

In 3+1 dimensional gravity theory in asymptotical AdS_4 spacetime, the BF bound for the scalar is $m^2 \geq -9/4$, so ν is always non-negative. For $\nu = 0$, the two terms $\psi_\pm$ will be degenerate and a new logarithmic term appears. We will not consider this case for simplicity. For $\nu \in (0,1]$, both modes $\psi_\pm$ are

normalizable. We can choose either ψ_+ or ψ_- as the source and treat the other as the corresponding response, and the dual operators are $\mathcal{O}_-$ and $\mathcal{O}_+$ respectively. We can calculate the retarded Green's function for the two operators respectively [291, 292],

$$G^R_{\mathcal{O}^\dagger_- \mathcal{O}_-} \sim \frac{\psi_-}{\psi_+}, \qquad G^R_{\mathcal{O}^\dagger_+ \mathcal{O}_+} \sim \frac{\psi_+}{\psi_-}. \tag{6.30}$$

When $w/T \to \infty$, the Green's function approaches the form in pure AdS_4 spactime, i.e. $G^R_{\mathcal{O}^\dagger_- \mathcal{O}_-} \sim 1/w^{2\nu}$ and $G^R_{\mathcal{O}^\dagger_+ \mathcal{O}_+} \sim w^{2\nu}$. For $\nu > 1$, only ψ_+ is normalizable. We can only take ψ_- as the source and treat ψ_+ as the corresponding response. The dual operator is $\mathcal{O}_+$ and we can calculate the retarded Green's function for it as above.

We notice from the equation of motion (6.27) and the infalling boundary condition (6.28) for ψ, the holographic superconductor has the symmetry $\chi_q(\omega) = \chi^*_{-q}(-\omega)$. For $q \neq 0$, one generally has $\chi''_q(\omega) \neq -\chi''_q(-\omega)$, and only for very high temperatures, the symmetry $\chi''(\omega) = -\chi''(-\omega)$ is restored. For the three models we considered in the last section, one always has $\chi''(\omega) = -\chi''(-\omega)$. We regard this as an artifact of the present minimal model of holographic superconductors. It would be interesting to see how the particle-hole symmetry can emerge in such holographic models.

6.5 Evolution of the full pair susceptibility

Using a SIN tunneling junction, experimentalists can measure the imaginary part of the full dynamical pair susceptibility χ''_p in the normal state of the quantum critical metals. In this section we investigate in detail theoretically the temperature and frequency evolution of $\chi''_p(\omega, T)$ for the three different scenarios introduced in the last section. We intend to use these models as templates that can be compared with future experimental results. Let us imagine what the experimentalists will do. They will take a sample, say some heavy fermion compound, tune it to the critical state by applying pressure or doping, scan the tunneling current for various bias voltages at different temperatures, and finally subtract the quasiparticle contributions to get the pair tunneling part. The superconducting transition temperature is fixed for this particular sample. So in our calculation, we will choose some particular sets of parameters, i.e., retardation scale, glue strength, etc., so that the three different models produce the same T_c. The overall magnitude of the measured $\chi''_p(\omega, T)$ depends on the details of the tunneling junction and is therefore difficult to predict on an absolute scale. The good news is that the difference of the various models also lies in the pattern of the relative change of the amplitude with frequency and temperature. So in the following study, we will normalize the amplitude with respect to its value at some particular reference temperature and frequency, and consider the quantity $\chi''_p(\omega, T)/\chi''_p(\omega^*, T^*)$.

For the three models with electron-glue dualism, we have formulated the equations in Matsubara frequency. Generically though, to obtain the real-frequency dynamical pair susceptibility, a crucial step is the analytic continuation, i.e., the replacement $i\Omega \to \omega + i\delta$, which is generally a non-trivial procedure. We choose the method of Padé approximants. Historically the Padé approximant analytic continuation method is based on continued fractions but the method of matrix inversion actually works much faster. Although the Padé approximant method is uncontrolled it seems to work very well in our case, probably because the pair susceptibility is a very smooth function with only a single characteristic peak/feature. Furthermore, our calculation has no statistical noise (it is not quantum Monte-Carlo), and in principle we can improve the precision arbitrarily by (i) increasing matrix size, (ii) increasing numerical precision in all steps, and (iii) increasing the number of Padé points $i\Omega_n$, until computational resources run out.

With the form of $\Gamma_0(i\nu_n; i\Omega)$ and $\lambda(i\Omega)$ specified as in Eqs. (6.8,6.16,6.20) and (6.13,6.14), we proceed to solve the Bethe-Salpeter equation (6.5) for the three different models, using matrix inversion to get $\Gamma(i\nu_n; i\Omega)$. Then we sum over ν_n and arrive at the imaginary frequency pair susceptibility $\chi(i\Omega)$, the analytic continuation of which, by the method of Padé approximants, gives the final result for the dynamical pair susceptibility $\chi_p(\omega)$.

For holographic superconductors, we solve the differential equation 6.27 with the boundary condition 6.28 near the horizon, and then extract the two coefficients $\psi_\pm$ near the boundary. The ratio of the two gives the pair susceptibility.

Figure 6.4 displays the temperature and frequency evolution of the imaginary part of the full dynamical pair susceptibility $\chi_p''(\omega, T)$ for the four different models in a false-color plot. Here the UV cut-off scale is set to $\omega_c \equiv 1$. The exponents, coupling strengths and retardation scales are tuned to give the same $T_c = 0.01$ for all three models with electron-glue dualism. For Fermi liquid BCS, the parameters are $\omega_b = 0.2$, $g = 0.3667545$. For the critical glue model, $\gamma = 1/3$, $\Omega_0 = 0.00267089$ (matrix size is 1000, number of Padé points is 16). For quantum critical BCS, $\alpha = 1/2$, $\omega_b = 0.2$, $g = 0.2131115$. For holographic superconductor, $T_c = 0.1468$. For all the four models, the horizontal axis is normalized with respect to T_c. The labeling ω should be understood as $\omega/(100T_c)$.

There is stunning difference for the four different scenarios. For FLBCS, there is a clear division of a core part and an external part. The core part corresponds to the peak, which dies out quickly away from T_c. The external part comes from the electronic pair susceptibility. Extrapolating the 'external' contours from high temperatures to lower temperatures, one finds that they converge to a single point. This convergence is readily read off from the bare pair susceptibility $\chi_{p,0} \sim \tanh(\omega/4T)$, the contours of which converge to $T = 0$, or $\tau = -1$.

The contours of the full pair susceptibility in QCBCS, HS and CG are all self-similar. However in CG, they are of elliptic shape, which is totally different from the corresponding bare one. This is clear sign that the effects of the critical glue persists even at high temperatures. In QCBCS and HS, the contours of the

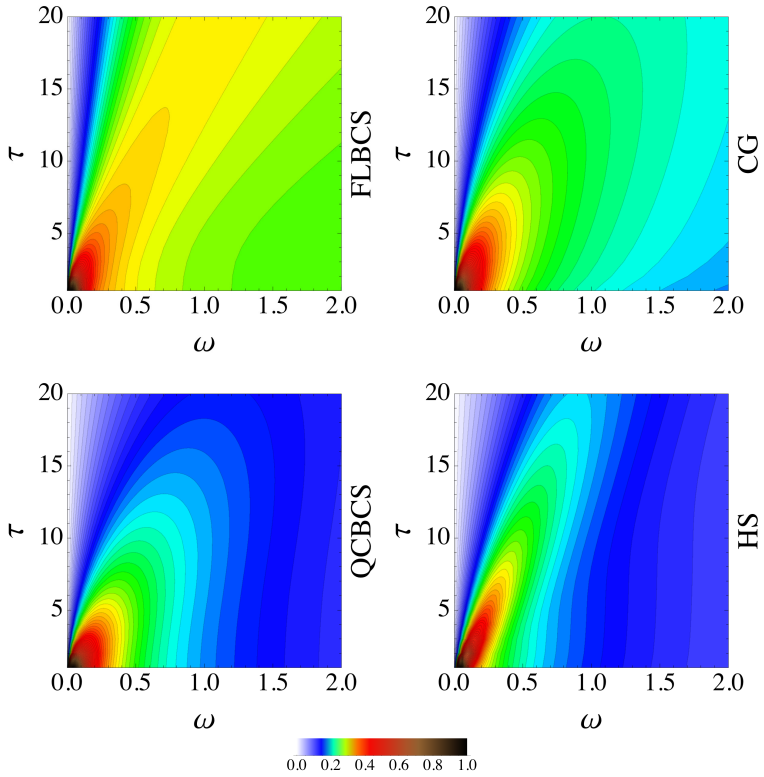

Figure 6.3: The imaginary part of the full pair susceptibility as function of frequency and temperatures for the three different models. Here we plot $\chi''(\omega,\tau)/\chi''(\omega_{\max},\tau=1)$. $\tau=(T-T_c)/T_c$ goes from 1 to 20. Frequency is normalized in terms of T_c, and the horizontal axis represents $\omega/(200T_c)$.

full pair susceptibility have the shape of a mountain with cliff on the right and they are quite similar to those of the bare ones, meaning that the electronic part dominates away from T_c.

Next we will consider linecuts of $\chi_p''(\omega,T)$ at various fixed temperatures. The gross feature is that for all the models considered, except the holographic superconductors with very small charge q, above T_c, $\chi_p''(\omega)$ always has just one peak. As temperature increases, the peak becomes broader, with the peak location moving to higher frequency, and the peak height decreasing. However the different models show subtle differences in the way how the peak changes with temperature. We will proceed to characterize the peak evolution, first near T_c and then away from T_c.

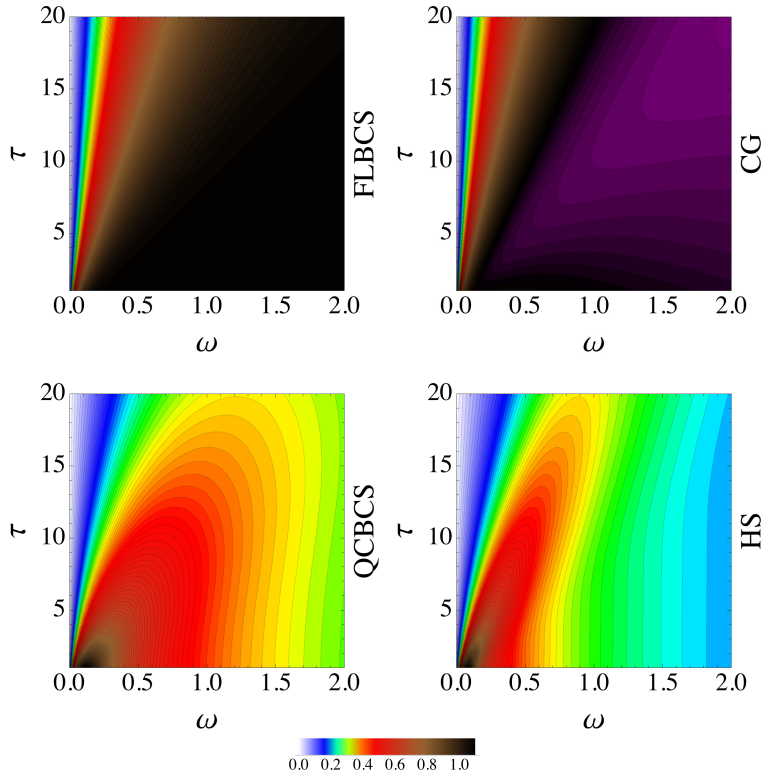

Figure 6.4: The imaginary part of the bare pair susceptibility as function of frequency and temperatures for the three different models. For holographic superconductor, we plot the corresponding result in Schwarzschild-AdS background.

For holographic superconductors with q near zero, we find that on top of the conformal peak, which has its origin from the asymptotic AdS geometry and thus insensitive to temperature, another peak gradually builds up as one approaches T_c. And in the temperature range $T_c < T \lesssim 5T_c$, we observe a peak-dip-hump structure plus the conformal tail at high frequencies.

The behavior of the pair susceptibility near T_c characterizes the nature of the superconducting transition. Here in the three models with electron-glue dualism, aiming at optimally doped cuprates as well as heavy fermion systems, we assume a mean field type transition, ignoring phase fluctuations altogether. The pairing fluctuations near T_c are thus diffusive in nature, and the pair susceptibility has a diffusive pole

$$\chi_p(\omega) \propto -N(0)T_c \frac{1}{i\omega - \tau_{\mathrm{GL}}^{-1}}. \tag{6.31}$$

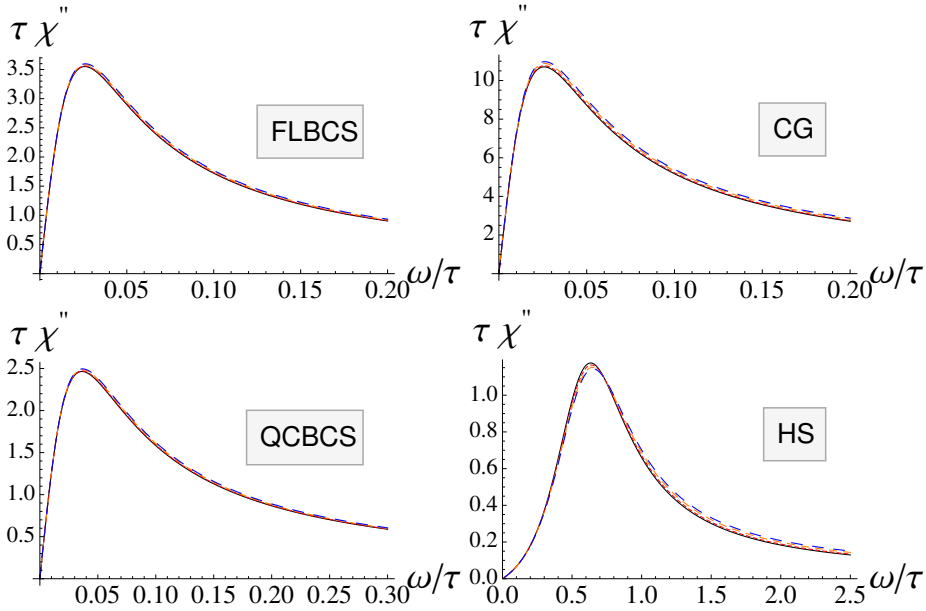

Figure 6.5: Scaling collapse of the imaginary part of the full pair susceptibility near T_c for the four different models: FLBCS, CG, QCBCS and Holographic superconductor. In each figure, we have plotted 4 different temperatures $T/T_c = 1.01, 1.03, 1.07, 1.1$.

Here the characteristic relaxation rate $\tau_{\rm GL}^{-1}$, stemming from pair breaking effects, can be determined from a Ginzburg-Landau calculation [277, 282]. Assuming preformed pairs above T_c would lead to a propagating nature for the pairing fluctuations and thus a different form of $\chi_p(\omega)$. But as already mentioned, we will not consider this possibility here. The proportionality factor in Eq. (6.31) is model dependent and for FLBCS is $8k_B/\lambda^2\pi\hbar$.

The immediate consequence of the diffusive pole in Eq. (6.31) is that near T_c the imaginary part of the pair susceptibility has a quasi-Lorentzian line-shape, i.e., a typical relaxational peak,

$$\chi_p''(\omega) \propto \frac{N(0)}{\tau} \frac{\omega\,\tau_{\rm GL}}{1+(\omega\,\tau_{\rm GL})^2}, \tag{6.32}$$

independent of the particular pairing mechanism. Here we have defined the reduced temperature $\tau = (T - T_c)/T_c$.

The peak evolution thus shows universal quasi-Lorentzian peak behavior near T_c for these three models. The peak location is at $\omega_{\rm max} \simeq \tau_{\rm GL}^{-1} \propto (T - T_c)$, which goes to 0 linearly as $T \to T_c$. The peak height is $\chi''_{p,\rm max} \propto N(0)T_c/(T - T_c)$,

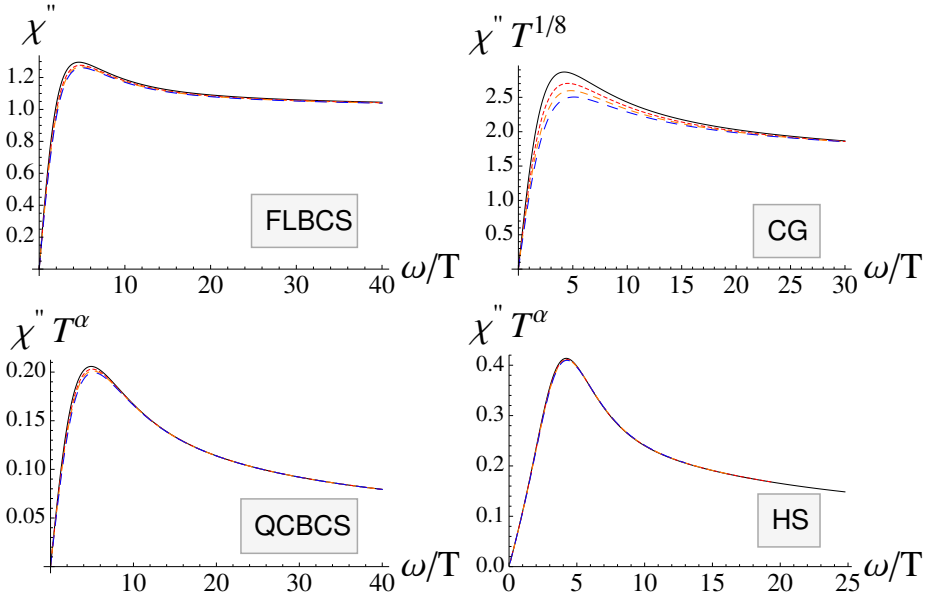

Figure 6.6: Scaling collapse of the imaginary part of the full pair susceptibility at high temperatures for the four different models: FLBCS, CG, QCBCS and holographic superconductor (from top to bottom). In each figure, we have plotted 4 different temperatures: $T/T_c = 11, 14, 17, 21$.

which diverges as $(T - T_c)^{-1}$ when $T \to T_c$. The full width at half maximum of the peak width is $\omega_{\rm wid} = 2\sqrt{3}\,\omega_{\rm max}$, which also vanishes linearly as $T \to T_c$. The fact that peak width and the peak location move together is a robust property of the peak and is used as self consistency check of our numerical calculations.

Above we wrote $\omega_{\rm max} \simeq \tau_{\rm GL}^{-1}$, and this was meant literally: in our numerical results we never find the *exact* relation $\omega_{\rm max} = \frac{8k_B}{\pi\hbar}(T - T_c)$. Instead, we find deviations from this result up to 10 percent for the FLBCS and CG models, and up to factor 3 difference for the QCBCS model. So, although the relaxational peak itself is universal for these three models, the precise location of the peak $\omega_{\rm max}$ does have some model-dependent information. Furthermore, the peak location $\omega_{\rm max}$ can be measured experimentally *without fitting , i.e., parameter free.* Unfortunately, the precise value of $\omega_{\rm max}$ depends also on non-universal parameters such as the glue coupling strengthλ. The only conclusive outcome that may arise is that if $\omega_{\rm max}$ *differs* from $\tau_{\rm GL}^{-1}$ by a factor of 1.5 or more, then the FLBCS and CG models are very improbable.

For holographic superconductor, as one approaches T_c, the pair susceptibility

becomes of the form

$$\chi_p(\omega) = \frac{\chi^{(0)}}{1 - i\omega\tau_1 - \omega\tau_2}, \tag{6.33}$$

where $\chi^{(0)}$ is frequency independent and diverges when approaching T_c. τ_1, τ_2 are real numbers and both of them diverge as $T \to T_c$, $\tau_1 = A_1/(T - T_c), \tau_2 = A_2/(T - T_c)$. The ratio A_1/A_2 is of order 1 even at T_c. In addition to the obvious frequency asymmetry, one can see the difference of the holographic superconductor with the other three models from the shape of the peak at positive frequencies near T_c (Fig. 6.5).

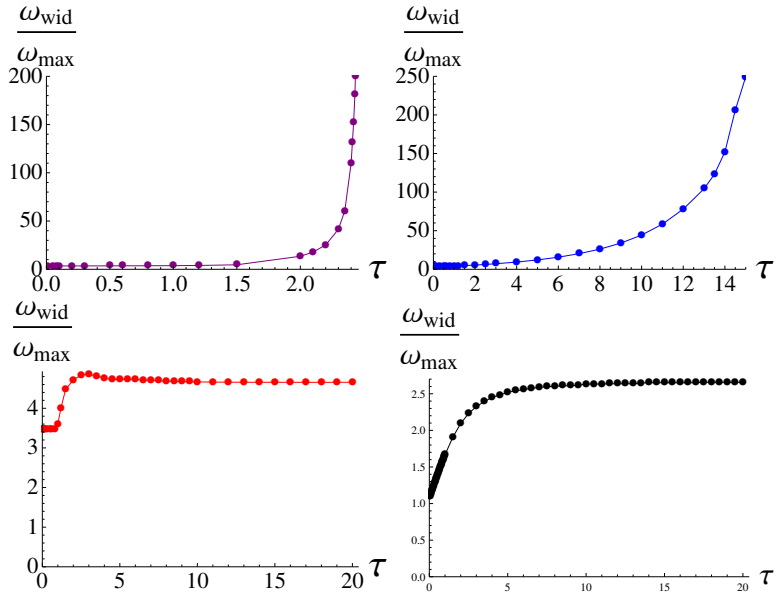

Figure 6.7: Evolution of the ratio of the peak width and peak location for Fermi liquid BCS (top left), Critical Glue (top right), QCBCS (bottom left) and holographic superconductor (bottom right).

Away from T_c, the pair susceptibility probes the normal state properties of the system, revealing the particular underlying pairing mechanisms. Different models give different predictions for the behavior of $\chi_p''(\omega)$ and the pair tunneling measurement can be used to further distinguish between the different models. The results for the four models introduced in the last section are shown in Figs. 6.6, 6.7.

The basic picture is that for the quantum critical BCS and holographic superconductors, the relaxational peak will cross over to the quantum critical peak originated from the electronic part of the pair susceptibility, while for Fermi liquid BCS and critical glue model, the peak simply dies out, and $\chi_p''(\omega)$ becomes

more and more flat at higher and higher temperatures. We plot in Fig. 6.6 the scaling collapse of the pair susceptibility. Scale invariance is spoiled by perturbative corrections in the critical glue model, and it does not have a good scaling collapse. The best-fit exponent actually changes as one fits different frequency ranges. All the other three models do have ω/T scaling. Another obvious feature one can read off from Fig. 6.6 is that the pair susceptibility in QCBCS and HS is more peaky than the other two models.

Such difference can be shown quantitatively by extracting the evolution of the peak location, peak height and peak width. The most revealing quantity is the ratio of the peak width and peak location (Figs. 6.7). For FLBCS and CG, the width and also the ratio grows exponentially at higher temperatures. For QCBCS and holographic superconductors, both the peak width and peak location increases linearly with temperature, and they are locked together again at high temperature, as they were in the region near T_c. We can see clearly in the ratio of the two, the crossover from one region dominated by the relaxational peak to a plateau dominated by the quantum critical peak. The behavior of the peak height in QCBCS and holographic superconductor is also quite different from the other two models. At high temperature, the peak height tends to a constant in FLBCS and CG, while for QCBCS and holographic superconductor it decays as power-law with exponent α_p, $\chi''_{p,\max} \sim T^{-\alpha_p}$. These will be the smoking gun evidences for QCBCS/HS.

6.6 Outlook: towards a realistic experiment

We have proposed to use the the second-order Josephson effect in SIN junctions to measure the pair susceptibility of the quantum critical metals. There are two possible experimental approaches using modern thin-film preparations and STM/STS techniques with a superconducting tip. Recently there has been significant progress employing multi-target pulsed laser deposition (PLD) to grow epitaxial layers of complex (ternary, quarternary , etc.) compounds [283]. Here the grand challenge would be to form a a tunnel junction between a high-temperature superconductor (HTS) and a heavy-fermion superconductor(HFS). For example, as proof of principal we suggest YBCO with $T_c = 90K$ and $CeIrIn_5$ with $T_c = 0.4K$ and the quantum critical region persisting to about 30K, both probably d-wave superconductors. With the enormous spread in transition temperatures one could thereby reach τ-values of about 70 over a wide range of frequencies ω at the lower temperatures. The advantage of HF-$CeIrIn_5$ is that around ambient pressures the superconducting dome is surrounded by regime of quantum critical behavior [293].

A second innovative method, now in development, is the scanning tunneling (STM/STS) measurement which has just been demonstrated as striking effective in probing the gap formations of URu_2Si_2 [294, 295]. We would suggest using a superconducting tip formed from the HTS either by etching down a single crystal

or gluing tiny crystallites of YBCO to a normal Ir or Pt tip. Such scanning experiments have never been attempted between a HTS and the cleaved surface of a HFS, e.g. $CeIrIn_5$, another grand challenge for the heavy fermion community. Stimulated by our pair-susceptibility calculations, we hope the experimentalists will evaluate the above possibilities in their efforts toward novel thin film and tunneling investigations.